Silicon Micromachined Pressure Sensors

K. N. Bhat

Abstract | Silicon micromachining for realizing micro mechanical structures has received considerable interest due to the several advantages of this technology over the conventional machining techniques. Silicon pressure sensors were the first micro mechanical transducers developed. Since then the market for micromachined pressure sensors has grown in leaps and bounds and found application in all walks of life including defense and space applications. The relevant micromachining technology and the design considerations are reviewed in this paper. The paper also gives the latest developments in this area and gives the details of the polysilicon piezoresistor based pressure sensors with Silicon On Insulator (SOI) approach for integrating pressure sensor and associated electronics.

Visiting Professor, ECE Department Indian Institute of Science Bangalore-560 012, India. [Formerly Professor of Electrical Engineering and coordinator of Microelectronics and MEMS research at IIT Madras, Chennai-600 036]

Piezoresistor: "piezo" is derived from the Greek word "piezen" meaning "to press". Piezoresistor is the resistor whose resistivity changes with pressure or stress.

1. Introduction

The Micro-fabrication technology, which has been the key to the success of microchips and microelectronics, is now revolutionizing the mechanical systems. Using this technology, basic mechanical devices such as motors, gears, bearings and springs have been miniaturized and integrated on silicon chips. The miniaturization of mechanical components promises to bring some of the same benefits to mechanical systems that microfabrication brought to electronics. Micro-mechanical devices and systems are inherently smaller, lighter and faster than their macroscopic counterparts and are often more precise. Since the devices are fabricated with the microfabrication techniques, they can be integrated with electronics to develop high-performance closed-loop-controlled Micro Electromechanical Systems (MEMS).

MEMS in general could consist of mechanical components, sensors, actuators, and electronics, all integrated in the same environment. The information provided by the sensors would be processed by the electronics whose output is fed to the actuators to manipulate the environment for the desired purpose. Over a decade ago, hundreds of MEMS components were prototyped and dozens were commercially available. However, many people then viewed the technology as the classical "solution looking for a problem to solve". The situation changed markedly during the 1990s, when the market for MEMS took off in a manner reminiscent of the growth in sales of integrated circuits in the 1960s. At present, over 100 million MEMS components are being sold annually.[1] The integrated sensors are currently the largest application of MEMS. Other demonstrated MEMS applications include flow valves, electromechanical switches and relays, gyroscopes, inkjet nozzles, micro-manipulators and connectors, as well as optical components such as gratings, wave guides, mirrors, sources and detectors.[2] For instance, a chip that contained over two million tiny mirrors, each individually addressed and moved by electrostatic actuation, has been produced by Texas Instruments and is commercialized in projection displays.[3]

Micromachining of silicon is a mature technology and the use of micro sensors for pressure, acceleration, angular rate and fluid flow is increasing at a high rate. They find wide application in the field of automobiles, process control, in the medical field and scientific instrumentation. These micromechanical devices consist of miniaturized mechanical structures with dimensions of micrometers to millimeters. The operation of micro mechanical sensor is based on the movement of a mechanical structure due to

Table 1: Mechanical properties of some of the materials

Material	Yeild Strength (GPa)	Knoop Hardness (kg/mm^2)	Young's Modulus (GPa)	Density (g/cm^3)
Diamond*	53	7000	1035	3.5
SiC*	21	2480	700	3.2
TiC*	20	2470	497	4.9
Al_2O_3*	15.4	2100	530	4.0
Si_3N_4*	14	3486	385	3.1
Iron*	12.6	400	196	7.8
SiO_2 (fibers)	8.4	820	73	2.5
Si*	**7.0**	**850**	**190**	**2.3**
Steel (max. strength)	4.2	1500	210	7.9
W	4.0	485	410	19.3
Stainless steel	2.1	660	200	7.9
Mo	2.1	275	343	10.3
Al	0.17	130	70	**2.7**

*Single Crystal
$1Pa = 1N/m^2 = 10\ dynes/cm^2$

MEMS: These are devices which have mechanical devices/structures dimensions in the microns range and also microelectronics devices.

CMOS: Complementary Metal Oxide Semiconductor (CMOS) transistor circuit is the basic circuit element used in the present day VLSI circuits.

Piezoelectric material: develops electric charges when subjected to stress (pressure). Piezoelectric pressure sensor makes use of this property to sense the pressure.

the effects of the pressure or acceleration etc with a mechanism to sense the motion of the structure to give an electrical output. The mechanical deformation due to mechanical forces and pressure can be measured using piezoelectric sensors, or by sensing the change in resistance due to piezoresistive effect or by noting the change in the capacitance of a capacitive sensor. High performance, high strength and high reliability materials are required for mechanical elements. Therefore, in this paper the mechanical properties of silicon are first highlighted to illustrate that silicon is one of the ideal materials for realizing MEMS structures and micromachined mechanical sensors followed by a discussion on the micromachining techniques for realizing mechanical components with accuracies down to micron level. A brief account of the various sensing techniques with reference to pressure sensors is presented in the subsequent section with emphasis on the piezoresitive pressure sensors, which are simple and hence are commercially very popular. The design considerations for a pressure sensor and the process details for realizing silicon membranes using the conventional approaches and the Silicon on Insulator (SOI) approach are next addressed. The merits of polysilicon piezoresistors for integrated pressure sensors are considered and the possibility of integrating pressure sensors with electronics on a monolithic silicon chip is demonstrated for the first time in India using SOI technique.

2. Silicon as a mechanical material

Silicon micromachining offers several advantages over the conventional machining techniques, the most important among them being the ability to batch process silicon wafers for fabricating mechanical devices such as sensors, actuators and microstructures having micron size details in the range of 1 to 10 microns. This also gives the added ability to integrate electronics with the micromachined mechanical devices.

Silicon also happens to be an ideal material for mechanical sensors because of its excellent mechanical properties required for reproducible elastic deformations under identical mechanical load. Silicon meets with these needs of mechanical structures because it is free of hysteresis and creep. Hysteresis is due to yield of the material, i.e., due to plastic deformation. Silicon, being a brittle material, does not deform plastically but it undergoes catastrophic failure when subjected to its ultimate yield strength of a few GPa. This stress at which silicon fails is considerably larger than the yield strength of stainless steel.

Creep is a phenomenon shown by almost all materials wherein a structure continues to deform under constant external load even if the load is considerably below the yield strength throughout the structure. Single crystal silicon is the best material to realize mechanical structure which is free from creep. The effects are ten parts per million.

Table 1 gives the mechanical properties of silicon[4] and several other materials. Figure 1 gives the elastic modulus and hardness of a variety of hard materials[5]. It can be seen that diamond has the highest hardness (100 GPa) and elastic modulus (1100 GPa). The extreme wear resistance up to 10,000 times greater than Silicon. However the primary challenge with diamond lies in integrating the mechanical devices with electronics. This is further complicated by the chemical inertness of diamond making it a difficult material to machine. Similarly, silicon carbide has drawn attention for MEMS because it offers much higher stiffness, hardness, toughness and wear-resistance than the core CMOS material. However it is also a difficult material to process due to its relatively very low chemical reactivity, extremely high melting point (2300°C). In spite of these difficulties, silicon carbide based MEMS pressure sensor has been successfully fabricated and reported in the literature[6].

Silicon crystal is of same type as diamond and is harder than most metals and has higher elastic limits than steel in both tension and compression. It can also be seen that silicon is harder than steel and lighter than aluminium. Furthermore silicon has the advantage that it is used as an electronic material in an already advanced VLSI technology. Therefore, miniaturized mechanical devices can be realized on silicon with high precision and they can be integrated with electronics. Miniaturization offers several advantages in mechanical sensors. For instance scaled down acceleration sensors can be used to sense higher accelerations. This is possible

Figure 1: Hardness and elastic modulus of a variety of hard materials[5]

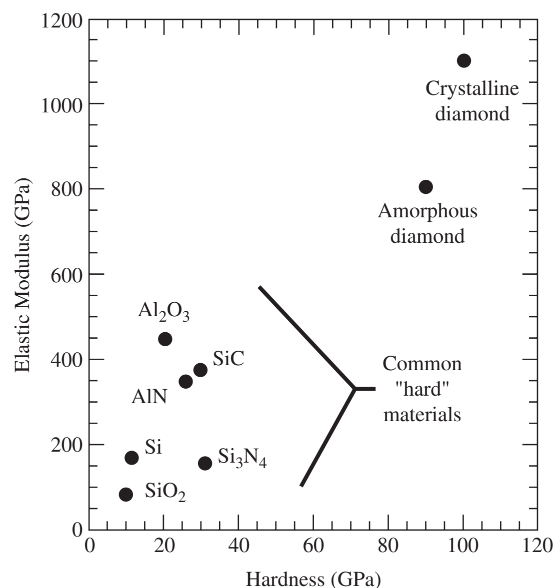

Breakdown strength: This is the electric field strength at which the dielectric material or a device fails to block the voltage and the current flow through it increases without having to increase the voltage. This is generally expressed as Volts per micron .0. (1 micron is 10^{-4} cm)

LIGA: is an acronym that stands for the main steps of its process deep X-ray **li**thography, electroplating (or ***g****alvo* in German) and injection moulding (or ***a****bformung* in German).

(100), (111): are the specified to identify a particular arrangement of atoms on the crystal surface . The [100] direction is perpendicular to the (100) plane.

holes: In semiconductors, current flow is due to the transport of two types of mobile charges. In simple terms, (i) electrons are mobile carriers having negative charge, (ii) holes are mobile carriers having positive charges.

because for a given acceleration, force which is proportional to mass scales down as the cube of the scaling factor, 'L' and hence the stress (Force per unit area) scales down linearly with scale factor 'L'.

Miniaturization with silicon provides additional benefits as follows. First, processing routes such as deposition, etching and diffusion limited doping etc., primarily act on surfaces are more economically attractive at small scales due to the cube-square scaling of volume to surface area. Secondly, electrostatic actuation force can be increased by about two orders of magnitude by scaling because the breakdown strength increases from 3 volts/μm (30 kV/cm) to 100 volts/μm when the air gap is reduced close to make free path of air molecule almost equal to 1 μm.

The basis of silicon micromachining is photolithography. The silicon micromachining includes etching, doping and deposition of thin films to fabricate three-dimensional structures with complex forms using wafer bonding and Deep Reactive Ion Etching. The micromachining processes[2] belong to three main categories, namely, (1) Bulk micromachining, (2) Surface Micromachining and (3) LIGA process. Among them the first two processes are widely used techniques in practice and therefore are presented in the following section.

3. Silicon micromachining based on lithography

Photolithography defines regions on silicon wafers where machining is done. In a bulk micromachining process shown in Fig. 2, material from the regions defined by photolithography is etched out to realize the required structures. For instance, cavities, holes and diaphragms as shown in Fig. 2 can be precisely fabricated by anisotropic etching silicon through a window opened in oxide by photolithography. The window size can be precisely controlled by lithography. The anisotropic etching process proceeds along the <100> direction and the boundaries of the etched portion are precisely guided by the (111) crystal planes as shown in the figure. As this plane is oriented at 54.7 ° to the (100) surface, the cavity depth is 0.7 W where 'W' is the width of the window.

When the width of the window opening is greater than $\sqrt{2}$ times the thickness of silicon wafer, a precise hole suitable for applications such as inkjet printer head can be fabricated. When the opposite side of the wafer is heavily doped with boron up to a depth '*d*', a diaphragm of thickness 'd' can be realized (see Fig. 2(b)) by etching through a square window of size $W = \sqrt{2}t + D$ where D is the dimensions of the side of the square diaphragm, and 't' is the thickness of the silicon wafer.

A precise hole of the required width 'h' can be realized by opening a window of width $H = \sqrt{2}t + h$. This also is shown in Fig. 2(b). Here the wider side is the surface on which the window is opened in the oxide or nitride which is used as a mask during the anisotropic etching process.

In the second approach for micromachining of silicon, namely, the surface micromachining technique, the structural layer, usually polycrystalline *silicon* is first deposited on an oxide layer grown on a silicon substrate. This structural layer is etched to realize the pattern. The oxide layer below this patterned structure is called the sacrificial layer because this layer is etched to release the structural layer. Fig. 3 illustrates this technique to fabricate a cantilever beam of polycrystalline silicon.

4. Brief outline of different types of pressure sensors

The first sensor fabricated using micro machining technique was the pressure sensor. They are now widely used for aerospace, biomedical, automobile and defence applications[7]. In general, pressure sensors are based on measuring the mechanical deformation caused in a membrane when it experiences stress due to pressure being sensed. Silicon is brittle and will break at a maximum strain of 2%. However, Young's modulus is very high (190 GPa) and below this elastic limit strain is linearly related to stress. The resulting strain or displacement is converted to electrical signals.

Figure 2: A schematic drawing of the basic concepts of bulk micromachining.

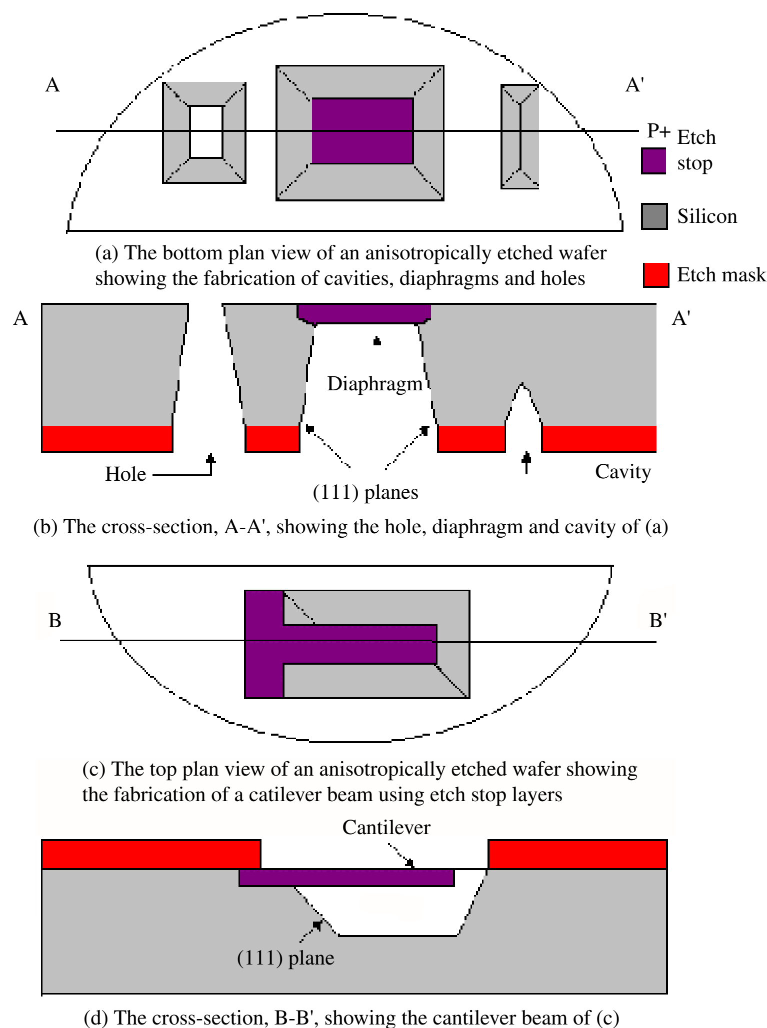

Polycrystalline silicon: is silicon made up of regions of different orientation. Each region is called as a grain and the region between the grains is called the grain boundary.

Principles used to sense strain are piezoelectricity, changes of electrical resistance due to geometric changes or piezoresistivity, changes in capacitance, changes in resonant frequency of vibrating elements in the structure or changes of optical resonance.

Silicon is not piezoelectric. Therefore in order to translate the deformation or strain into electrical signal with this approach, it is necessary to externally glue a piezoelectric pellet on the membrane. This technique does not form part of the conventional integrated circuit technology. Furthermore, the *piezoelectric* pressure sensors cannot be used for static pressure sensing purposes due to charge leakage.

The capacitive pressure sensor detects the deflection of the membrane as a variation in capacitance between two plates. The output of a capacitive pressure sensor is a change in capacitance, which has to be converted in to electrical signal using additional electronic circuits. The output of a capacitive pressure sensor is not linear with respect to the applied pressure. However, they have high sensitivity and are not sensitive to temperature[8].

The use of strain gauges is very common in conventional pressure sensors. These sensors make use of the change in the resistance of conductors due to the change in their physical dimensions when subjected to strain. When assembled on a membrane they give information about the strain experienced by the membrane when it is subjected to stress by the applied pressure. When the resistors are made of semiconductors, the change in the resistance is predominantly due to the change in the resistivity. This effect is known as the piezoresistivity and it is a phenomenon by which the electrical resistance of a material changes in response to mechanical stress. In the Piezoresistive pressure sensors semiconductor resistors are laid out on a membrane to sense the strain from the membrane that is subjected to external pressure. The first application of piezoresistive effect was in metal strain gauges to measure strain. In 1954, Smith[9] reported that silicon and germanium had much greater piezoresistive effect than metals. The discovery of the piezoresistive effect in silicon and germanium in 1954 has been commonly cited as the stimulus for silicon based sensors and micromachining. The first piezoresistive pressure sensor based on diffused resistors in thin silicon diaphragm was demonstrated in 1969. A vast majority of commercial pressure sensors today use piezoresistive sensing.

The vibration frequency of a mechanical beam or a membrane depends on the extent it is stretched. This is similar to the vibration frequency of a stringed musical instrument. This phenomenon has been used in conventional mechanical sensors which are classified as resonant sensors. As the output signal from a resonant sensor is a frequency, it can be easily transferred into a digital signal and interfaced with computer systems without having to use an A to D converter. These sensors are noted for their high stability and high resolution as a frequency signal is much more robust than an amplitude (e.g. a voltage). The stability is determined only by the mechanical properties of the resonator material, which is generally very stable. The disadvantage of resonant silicon sensors are that they are not easy to fabricate and hence become expensive. The high costs may be compensated by innovative simpler mechanical structures and by the simpler electronics.

Among the various micromacihned pressure sensors, the piezoresitive pressure sensors are the

Figure 3: Schematic demonstrating surface micromachining in its simplest form.

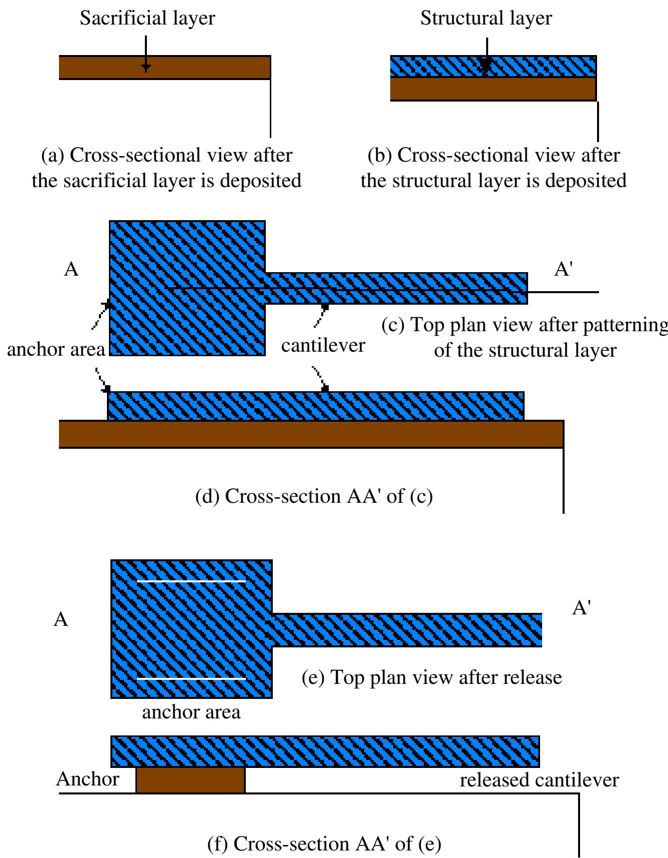

Effective mass: Both electrons and holes experience the effect of electric filed within the crystal and the external applied force due to applied electric field. The concept of effective mass for holes and electrons allows the use of classical Newton's laws of motion as follows: External applied force = effective mass × acceleration . The effective mass concept absorbs the effect of the internal forces acting on the particle within the crystal.

Mobility: When an electron or a hole is subjected to external field E, it acquires a steady state velocity v which is proportional to the electric applied field. The proportionality constant is called the mobility of the charged particle.

simplest to fabricate and provide electrical output directly. As will be seen in the subsequent sections, they can be easily integrated with microelectronics circuits because the fabrication processes are compatible with the integrated circuit fabrication techniques. Therefore, we focus our discussion on the piezoresistive pressure sensors.

5. Piezoresitive effect and gauge factor in single crystal silicon

5.1. *Piezoresistivity*

Piezoresistivity in silicon arises from the deformation of energy bands as a result of stress. The deformed bands affect the *effective mass* and consequently the *mobility* of electrons and *holes* and hence modifying the resistivity. The piezoresistive effect in P-type silicon can be understood by examining the Energy E versus momentum k band structure[10] shown in Fig. 4.

The valence band structure of silicon is composed of three bands: the heavy hole band, the light hole band, and the spin orbit split-off band. The first two bands are degenerated at $k = 0$. The spin orbit split off band is situated at energy 0.044 eV below. Consequently it is considerably depopulated compared to the heavy and light hole bands. The hole conductivity in silicon is given by

$$\sigma = q^2\Gamma\left(\frac{p_1}{m_1^*} + \frac{p_2}{m_2^*}\right) \quad (1)$$

where m_1^* and m_2^* are the effective masses in the heavy and light hole bands respectively, Γ is the relaxation time and p_1 and p_2 are the hole concentrations in the heavy and light hole bands respectively. The mobility and the effective mass (m^*) is related to the curvature of the E–k diagram by the following equation[11]

$$\mu \propto \frac{1}{m^*} \propto \frac{\partial^2 E}{\partial k^2} \quad (2)$$

From equations (1) and (2) it can be seen that the conductivity and hence the resistivity change can be affected by either changing the shape of a band or by changing the energy level of a band. For example, when a longitudinal tensile stress is applied on p-type silicon, the heavy and light hole valence bands will separate as shown in Fig. 4(b). The light hole band decreases in energy relative to the heavy hole band. This causes a population shift of holes from the light hole band to the heavy hole band where the mobility of holes is lower than in the light hole band. The heavy hole population increase leads to a decrease in mobility and an increase in resistivity. Effective mass change due to applied stress has two origins. The first one is due to the mixing between light hole and the spin orbit split off bands leading to mass shift for light holes. The second one due to the mass change effect is caused by the decrease of interaction between the heavy and light hole bands following the separation between the heavy hole and light hole bands.

5.2. *Piezoresistive Coefficients*

The resistance change can be calculated as a function of the stress using the concept of piezoresistive coefficient. There is a contribution to resistance change from stresses that are longitudinal (σ_l) and transverse (σ_t) with respect to the current flow. The fractional change in the resistance has a first order linear dependence on the stress in the lateral and longitudinal directions. Assuming that mechanical stresses are constant over the resistors, the relative resistance change ΔR is given by[12]

$$\frac{\Delta R}{R} = \sigma_l\pi_l + \sigma_t\pi_t \quad (3)$$

where π_l and π_t are the longitudinal and transverse piezoresistive coefficients, respectively and σ_l and

Figure 4: Valence band and energy surfaces in the k-space of (a) Unstressed silicon (b) Highly stressed silicon.

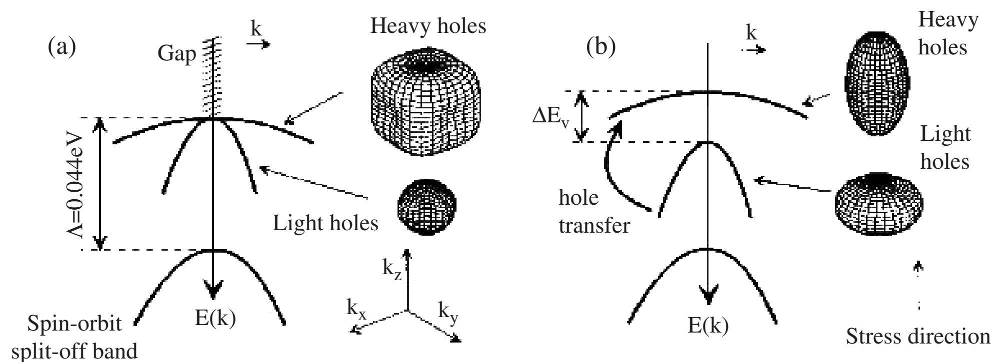

Doping concentration: is the impurity concentration that is introduced to the pure silicon to change the carrier concentration and hence the resistivity of silicon.

σ_t are the longitudinal stress and transverse stress respectively.

The piezoresistive coefficients depend upon the crystal orientation and can change significantly from one direction to other. They also strongly depend on dopant type and concentration, a reflection of the fact that detailed valence band and conduction band structures in silicon are very different for N-type and P-type material and are strong functions of doping concentration.

Table 2 shows piezoresistive coefficients for N-type and *P*-type (100) wafers and doping levels below 10^{18} cm^{-3}.[12,13] The values decrease at higher doping concentrations. For (100) wafers, the piezoresistive coefficients for *p*-type elements are maximal in the <110> directions and vanish along the <100> directions. Therefore p-type piezoresistors must be oriented along the <110> directions to measure stress.

5.3. *Gauge Factor*

The piezoresistive effect can be quantified using the gauge factor. The general definition for the gauge factor begins with the relationship between resistance R and resistivity, ρ. The resistance R of a rectangular conductor is expressed by

$$R = \frac{\rho_l}{wt} \tag{4}$$

Table 2: Piezoresistive coefficients for *P*-type and *N*-type (100) wafers and doping levels below 10^{18} cm^{-3}

	π_l (10^{-11} Pa^{-1})	π_t (10^{-11} Pa^{-1})	
P-type	0	0	in <100> direction
	72	−65	in <110> direction
N-type	−102	53	in <100> direction
	−32	0	in <110> direction

where ρ is the resistivity and l, w, and t are the length, width and thickness of the conductor respectively. When the resistor is subjected to strain, the relative change in resistance is given by[14]

$$\frac{\Delta R}{R} = \frac{\Delta l}{l} - \frac{\Delta w}{w} - \frac{\Delta t}{t} + \frac{\Delta \rho}{\rho} \tag{5}$$

Here Δl, Δw, Δt and $\Delta \rho$ are the changes in the respective parameters due to the strain. If the resistors experience tensile stress along the length, the thickness and width of the resistor will decrease whereas the length will increase. Poisson's ratio, ν, is used relate the change in length to the change in width and thickness of the piezoresistors by the following equation

$$\frac{\Delta w}{w} = \frac{\Delta t}{t} = -\nu \frac{\Delta l}{l} \tag{6}$$

The gauge factor G (strain sensitivity) is given by

$$G = \frac{\Delta R/R}{\varepsilon} = 1 + 2\nu + \frac{\Delta \rho/\rho}{\varepsilon} \tag{7}$$

where $\varepsilon = \frac{\Delta l}{l}$ is the strain. The first two terms in equation (7) represent the change in resistance due to dimensional changes and are dominant in metal gauges, while the last term is due to the change in resistivity. In semiconductor gauges, the resistivity change is larger than the dimensional change by a factor of about 50, and the dimensional change is generally neglected.

As shown in Table 3 below, the gauge factors of different types of strain gauges[8,15] can be vastly different due to mainly whether or not they have a significant piezoresistive effect as in the case of the semiconductors. For metals, ρ does not vary significantly with strain and ν is typically in

Table 3: Gauge factors of different types of strain gauges

Type of Strain Gauge	Gauge Factor
Metal Foil	1 to 5
Thin-Film Metal	≈2
Diffused Semiconductor	80 to 200
Polycrystalline Silicon	≈30

the range of 0.3 to 0.5, leading to gauge factors of only about two in the metal strain gauges. In semiconductor strain gauges, the piezoresistive effect is very large and hence the gauge factor is considerably high. Gauge factors up to 200 for P-type silicon and up to 140 for N-type silicon have been reported.

6. Single crystal piezoresistive pressure sensor

6.1. *Design with flat diaphragms*

The basic structure of a piezoresistive pressure sensor consists of four sense elements connected in a Wheatstone bridge configuration to measure stress in a thin, crystalline silicon membrane as shown in Fig. 5. With the advent of silicon bulk micromachining with anisotropic etching, the membranes are invariably rectangular or square and they are realized on (100) plane with the edges in the <110> directions. The stress is a direct consequence of the membrane deflection in response to an applied pressure. The design of a pressure sensor involves the thickness and geometrical dimensions of the membrane and the location of the piezoresistors on the membrane to achieve maximum sensitivity.

Figure 5: Schematic cross section and top view of a single crystal piezoresistive pressure sensor showing the P-type piezoresistors arrangement on a N-type membrane. The right side of the diagram shows the resistors in Wheatstone bridge connection.

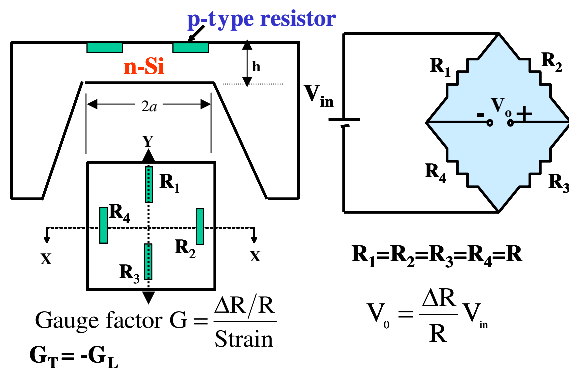

From the theory of elastic deformation on plates, the maximum deflection $w_0$of a square membrane of thickness h and side $2a$ takes place at the center of the plate and is related to the applied pressure,P, by the relationship given by the equation[16,17],

$$P = E\frac{h^4}{a^4}\left[g_1\frac{w_0}{h} + g_2\left(\frac{w_0}{h}\right)^3\right] \tag{8}$$

Here, E is the Young's modulus, g_1 and g_2 are related to the Poisson ratio and given by the equations,

$$ng_1 = \frac{4.13}{1-\nu^2}, \quad \text{and} \quad g_2 = \frac{1.98(1-0.585\nu)}{1-\nu} \tag{9}$$

In equation (8) the first term is due to the stress distribution caused by pure bending that is the central plane of the diaphragm is not stretched or compressed. This is true if the deflection of the diaphragm is small compared to its thickness. If the deflection of the diaphragm is not small when compared to its thickness, the central plane of the diaphragm will be stretched as in a membrane. The second term in equation represents the stress caused by the stretch of the central plane. As it can be seen from equation (8) the second term is a source of nonlinearity in the piezoresitve pressure sensors. Therefore even though a reduction in the thickness h would increase the deflection w_0 and hence the sensitivity of the pressure sensor, it is necessary to keep h sufficiently thick so that w_0 at the maximum operation pressure is small when compared to h. The maximum burst pressure is second criterion for choosing the thickness of a diaphragm. This is defined as the pressure at which the diaphragm ruptures. The stress in a square diaphragm of side $2a$ is maximum at its edge center and is given by the relation,

$$\sigma_{\max} = P\left(\frac{a}{h}\right)^2 \tag{10}$$

Thus for a given value of $2a$, the thickness h should be chosen such that at the maximum operating pressure $P_{\max}$ of the sensor, $\sigma_{\max}$ estimated using equation (10) is less than the burst pressureσ_{burst}. For single crystal silicon ideal value of σ_{burst} is 7 GPa (1 Pa = 1 N/m^2 and 1 bar = 1 atmospheres = 10^5 Pa)

The next design criterion is to assign proper locations for the piezoresistors on the diaphragm so that the sensitivity is maximum using the diaphragm dimensions designed from the linearity and burst pressure considerations. In the case of single crystal piezoresistive pressure sensor design layout on (100) substrates, the four diffused P-type piezoresistive sense elements are located near the edge of the

diaphragm, as shown on the left side in Fig. 5, where the stress is maximum as given by equation (10).

Here the two piezoresistors R_1 and R_3 are placed perpendicular to opposite edges of the membrane, and the other two (R_2 and R_4) are placed parallel to the other two edges. When the membrane deflects downwards, causing tensile stress at the edges of the membrane surface, both the resistors R_1 and R_3 experience longitudinal stress σ_l and the transverse stress σ_t given by the relations,

$$\sigma_l = P\frac{a^2}{h^2}, \quad \text{and} \quad \sigma_t = \nu P\frac{a^2}{h^2} \qquad (11)$$

and hence show an increase in resistance ΔR given by the relation,

$$\frac{\Delta R}{R} = \pi_l P\frac{a^2}{h^2}(1-\nu) \qquad (12)$$

Similarly, the resistors R_2 and R_4 laid out parallel to the edge of the diaphragm experience transverse and longitudinal stresses given by,

$$\sigma_t = P\frac{a^2}{h^2}, \quad \text{and} \quad \sigma_l = \nu P\frac{a^2}{h^2} \qquad (13)$$

They show decease in resistance given by the relation

$$\frac{\Delta R}{R} = \pi_t P\frac{a^2}{h^2}(1-\nu) \qquad (14)$$

In single crystal (100) silicon, π_l and π_t are equal to each other in magnitude. Therefore, the absolute value of the four resistance changes can be made equal when the resistors are arranged in locations as shown in Fig. 5 and hence maximum sensitivity can be achieved. The resistors are chosen to be equal in magnitude so that the bridge is balanced when the pressure is zero. When the diaphragm is subjected to pressure due the unbalance created in the bridge results in an electrical output V_0 of polarity shown in the Fig. 5 and is given by the relation

$$V_0 = \frac{\Delta R}{R}V_{in} = P\frac{a^2}{h^2}(1-\nu)\,\pi\,V_{in} \qquad (15)$$

where R is the zero-stress resistance of each of the resistors and V_{in} is the bridge supply voltage.

Figure 6: Schematic view of twin island structure

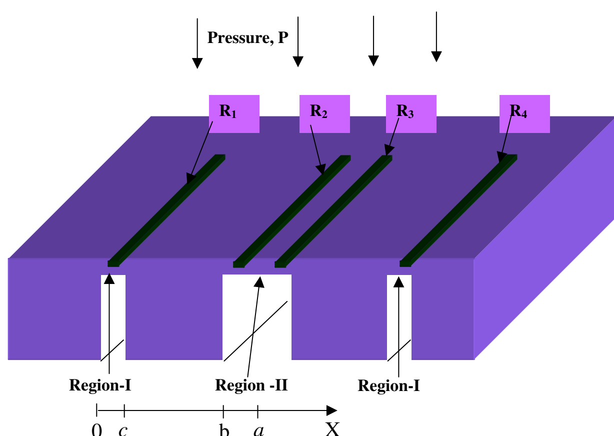

6.2. *Pressure Sensors with sculptured diaphragm or bossed diaphragm structures*

In low pressure range (e.g., a full-scale pressure of about 500 Pa), flat-diagram pressure sensors are not suitable because the sensitivity will have to be increased considerably by making the $(\frac{a}{h})$ ratio extremely large, resulting in high degree of nonlinearity. As discussed before, the nonlinearity is the result of stretching of the middle plane which becomes significant when the deflection becomes comparable to thickness of the diaphragm. In order to improve the sensitivity and the linearity simultaneously, specialized geometries such as diaphragms with a rigid center or boss[18] have been introduced for increasing the stiffness to limit the maximum deflection of the diaphragm, for enhancing the linearity. Such a structure has also been known as the sculptured structure and is schematically shown in Fig. 6.[18]

In this structure all the four resistors are subjected to transverse stress when the pressure is applied as shown in the Fig. 6. The resistors R_1 and R_4 (located in Regions-I) experience identical transverse tensile stress and are connected to the opposite arms of a Wheatstone bridge. The resistors R_2 and R_3 (located in the region-II) experience identical transverse compresive stress and are connected in the other opposite arms of the bridge. In this structure, the presence of the rigid island enhances the linearity because the stresses in the regions-I and II are quite balanced. At the same time this structure ensures high sensitivity due to the stress concentration in the regions where the piezoresistors are located. A detailed analysis of this structure shows[19] that the average stress in the region I (Region between 0 and c) is about $1.35P\frac{a^2}{h^2}$ and the average stress in the region II between b and a is $= -1.35P\frac{a^2}{h^2}$, and that the output voltage from the pressure sensor can be approximated by,

$$V_o = 1.5P\frac{a^2}{h^2}(1-\nu)\pi_t V_{in} \qquad (16)$$

Comparing V_0 in eqn (16) with that in equation (15) we can see that the sensitivity of the twin island

Figure 7: TCR of boron doped LPCVD polysilicon and single crystalline silicon as a function of doping concentration[20]

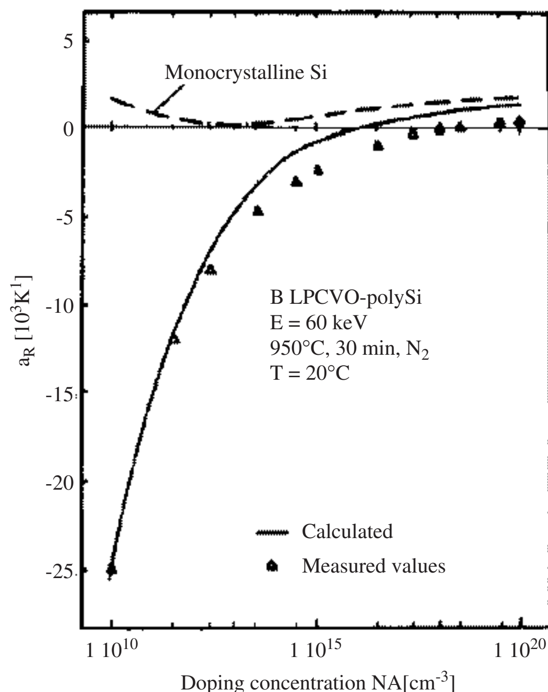

structure sensor is about 1.5 times higher than the sensor with a flat diaphragm. Simulation with ANSYS has also shown that the maximum displacement in this twin island structure is reduced by a factor of 2 compared to the flat diaphragm of same $\frac{a}{h}$ ratio.

7. Polycrystalline silicon pressure sensors

7.1. *Advantages of Polysilicon as Piezoresistive Material*

The general purpose piezoresistive pressure sensors are realized by arranging diffused or implanted *p*-type resistors in the form of a Wheatstone bridge on an n-type single crystalline diaphragm. The locations of the resistors on the diaphragm are at the four centers of the diaphragms edges, as discussed in the previous section. The isolation between these resistors is provided by the *p–n* junction, which is formed by the *P*-type resistors with the *N*-type membrane layer. The leakage current of a *p–n* junction increases exponentially with temperature. Therefore, the isolation between the resistors of the conventional piezoresistive pressure sensors becomes poor at temperatures in excess of about 100 °C. On the other hand in the case of polysilicon piezoresistive pressure sensors, polysilicon resistors are laid out on oxide grown on the diaphragm region and hence are isolated from each other by the oxide layer. Therefore isolation is maintained even at temperatures in excess of 300 °C. The total resistance of polysilicon is determined by the resistance of the silicon grains and that of the grain boundaries, the latter being the most important aspect. Within the grains, the current transport is by carrier drift and the resistivity of the grain region behaves essentially like that of the single crystal material. Therefore, as the mobility decreases at higher temperature, the resistivity of the grain region increases with temperature. On the other hand, at the grain boundaries, depletion regions develop due to the charge trapping and result in potential barriers for carrier transport. At higher temperatures, more carriers can overcome these barriers, and the grain boundary resistance decreases with temperature rise[20]. The barrier height at the grain boundary is a function of doping concentration. Therefore the temperature coefficient of resistivity (TCR) of polysilicon can be tailored and almost made nearly zero by adjusting the boron doping concentration[20] so that the positive TCR of the grains is balanced by the negative TCR of the grain boundary regions. Experimental results reported recently[21] on boron implanted LPCVD polysilicon resistors have shown that the TCR of LPCVD polysilicon can be educed to a value equal to $1.75 \times 10^{-5}/°K$ with the room temperature resistivity $\rho = 1.05 \times 10^{-2}\,\Omega - \text{cm}$ for the doping concentration $N_A = 2.66 \times 10^{19}/\text{cm}^3$.

Figure 7 shows the change in the temperature coefficient of single crystal silicon and that of polysilicon as a function of boron concentration N_A.[20] From the figure it can be seen that TCR of boron-doped LPCVD polysilicon resistors can be negative, approach zero, or be positive depending on the doping concentration. In contrast, the TCR of mono crystalline P-doped silicon as shown in Fig. 7 is always positive. For doping concentration greater than 3×10^{19} cm^{-3}, polysilicon have nearly zero TCR. However for single crystal silicon, N_A has to be carefully adjusted since TCR is zero only at particular N_A. Furthermore this N_A is low leading to higher values of resistance.

7.2. *Piezoresistive Properties of Polysilicon*

The piezoresistive effect in polysilicon film composed of many small crystal grains with different orientation originates from every grain. As discussed before, the carrier trap charges at the grain boundary create depleted layers on the grain. On the assumption that the grain boundary and depleted layer are insensitive to stress,[22] the non-depleted crystalline silicon in the grain makes average contribution in all possible directions to the piezoresistance of the polysilicon film. Therefore, the piezoresistive effect in polysilicon films is isotropic

Figure 8: Longitudinal and transverse gauge factors as a function of the doping Concentration of boron doped LPCVD polysilicon resistors.[23]

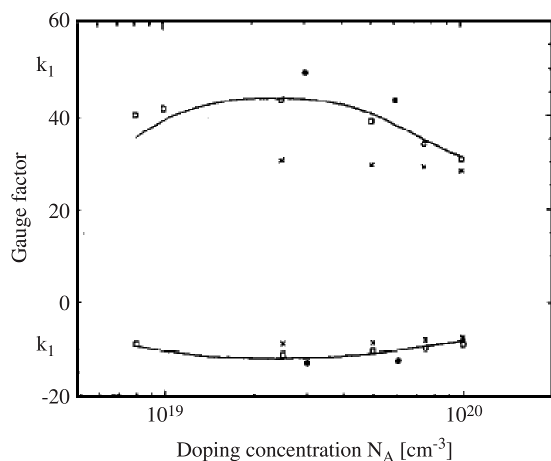

Figure 9: Different arrangement patterns of polysilicon resistors on membranes

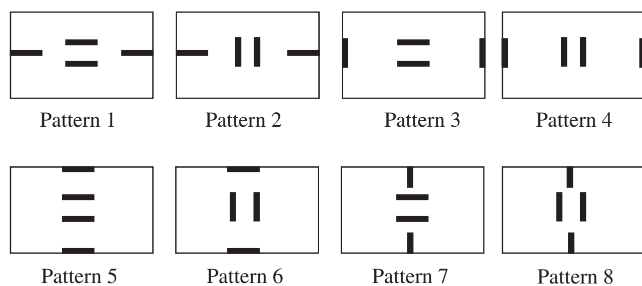

and is less than that of the single crystal silicon. The longitudinal gauge factor (G_L) of boron-implanted polysilicon is larger than the transverse gauge factor (G_T)[23] by a factor of about three as shown in Fig. 8. Therefore when polysilicon is used as piezoresistors they should be arranged in such a way that they should experience maximum longitudinal stress in order to achieve better sensitivity.

7.3. *Polysilicon Resistor Arrangement on the Diaphragm for Best Sensitivity*

The longitudinal effect of piezoresistance is preferred for polysilicon because G_L is larger than G_T. Therefore, the arrangement of polysilicon strain gauges needs to be different from the single crystal strain gauge arrangement to achieve best sensitivity values. A detailed simulation study has been reported[22] on this aspect using Finite Element Method to analyze the stress distribution on the rectangular membrane. This study demonstrated the following features: (i) stress concentration is high at the center and the areas near the middle edge of the membrane. The polysilicon strain gauges should be arranged into these areas, (ii) the deformation along the narrower direction is larger than that along the longer direction of the rectangular membrane. The polysilicon resistors should be arranged along the narrower direction to increase the sensitivity of sensors.

Several possible arrangement patterns of polysilicon resistors as shown by dark lines in Fig. 9 have been studied for different geometrical sizes of the membrane. The results[22] have shown the following: (1) The arrangement Pattern 8 shown in Fig 9 gives the best results in terms of maximizing the output voltage of the sensor because the piezoresistors are taking the advantage of longitudinal piezoresistive effect of polysilicon and placed along the narrower direction. (2) In the sensor design, the length to width ratio of the rectangular membrane should be increased to some degree to enhance the output.

For instance, the results of the study[22] predicted an output voltage of 32.89 mV with 5 volts input and 0.08 N/mm^2 stress on a $7 \times 3 \times 0.1$ mm^3 membrane as compared to 24.37 mV for a $4 \times 3 \times 0.1$ mm^3 membrane when the pattern 8 is used. Our simulation studies[24,25] using ANSYS showed that the piezoresistors located at the edges of the membrane undergo maximum longitudinal tensile stress and those located at the center of the membrane experience longitudinal compressive stress. The results of[24,25] also showed that the magnitudes of these longitudinal stresses at the edge and at the center increase and reach a maximum value when the diagram is rectangular with its length to width ratio takes a value of two as shown in Figs 10 and 11. Based on these studies, the polysilicon resistors are arranged in a Wheatstone bridge connection as shown in Fig. 12 on an oxidized rectangular diaphragm having an aspect ratio equal to two with the width equal to 500 μm.

7.4. *Design and fabrication of Polysilicon Piezoresistive pressure sensor with Silicon On Insulator (SOI) approach*

The schematic cross-section of polysilicon piezoresistive pressure sensor structure fabricated at the Indian Institute of Technology Madras, Chennai is shown in Fig 13. Based on the simulation results shown in Figs 10 and 11, rectangular membranes with different aspect ratios have been chosen and the resistors are arranged on the membrane as shown in Fig. 12 so that the resistors placed at the edges experience longitudinal tensile stress causing an increase in resistance and those placed around the

Figure 10: Longitudinal and transverse stress at the longer edge of the rectangular diaphragm, as a function of its length for fixed.

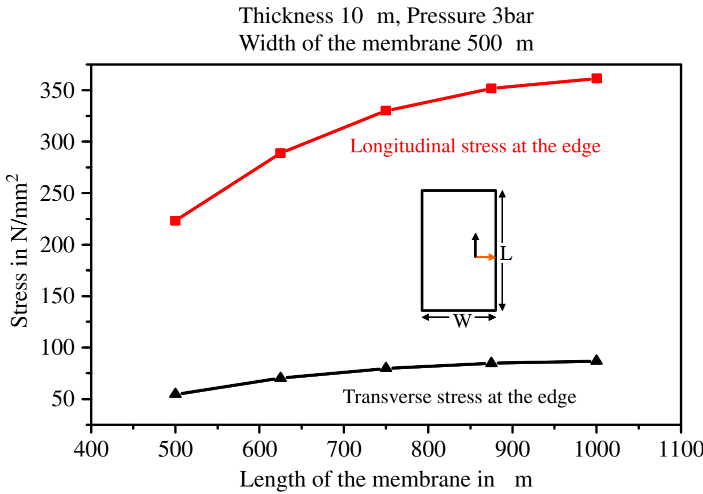

middle experience longitudinal compressive stress causing a reduction in the resistance value when the diaphragm is subjected to differential pressure. The resistor values are targeted to be around 1.0 kΩ so that the current drained by the bridge is within 10 mA when the input voltage is 10 Volts. The various process steps involved in the fabrication of polysilicon piezoresistive pressure sensors are realization of boron doped polysilicon resistors, connection of these resistors in a Wheatstone bridge network. The diaphragm is realized by bulk micromachining of SOI wafer. The SOI wafer is fabricated in-house in the Microelectronics laboratory at IIT Madras by Silicon Fusion Bonding (SFB) of oxidized silicon wafers and back etching the top wafer to reduce the thickness of the SOI layer so that it forms the diaphragm as shown in Fig. 13 at the end of the anisotropic etching step. The SOI approach is used to enable integration of electronics with the pressure sensor as will be illustrated in the next section.

The diaphragm thickness (SOI layer thickness) is chosen based on the burst pressure considerations. The burst pressures are estimated using the ANSYS for three different membrane thicknesses with different aspect ratios of the diaphragm. These results were generated taking an ideal value of rupture stress of 7 GPa. In practice, this has been reported to be lower than 7 GPa. Therefore, considering a safety factor of two, the membrane thickness is estimated to be 15 μm for a maximum pressure (P_{MAX}) of 10 Bar and a burst pressure of $5P_{\text{MAX}}$. Similarly, the membrane thickness is estimated to be about 10 to 11 μm for a maximum pressure P_{MAX} of three Bar and a burst pressure of $5P_{\text{MAX}}$.

7.5. *Results on the Discrete packaged Sensors*

Pressure sensors fabricated were packaged at Bharat Electronics Limited (BEL), Bangalore and tested at IIT Madras, Chennai at different pressure ranges and Temperatures. The Table 4 summarizes the results.

8. Important parameters of a pressure sensor

The most important parameters of the pressure sensor are the following.

(1) Sensitivity (S)

The pressure sensitivity (S) is defined as the relative change of output voltage per unit of applied pressure. This is expressed in mV/V-Bar.

$$S = \frac{\Delta V_0}{\Delta P}\frac{1}{V_{in}} = \frac{\Delta R}{\Delta P}\frac{1}{R} \tag{17}$$

It can be seen that sensitivity depends on $\Delta R/R$ which depends on the gauge factor. The sensitivity of the polysilicon pressure sensors is four to five times lower than that of the sensitivity of conventional single crystal piezoresistive pressure sensors. This is due to the lower value of the gauge factor of polysilicon piezoresistors. However the output and hence the sensitivity can be enhanced using an amplifier circuit which can be realized on chip as discussed in the following section, using the SOI approach.

(2) Offset voltage (V_{off})

The output voltage of the pressure sensor without any pressure being applied is called an offset voltage. This is due to mainly two reasons. The first one is due to some residual stress on the membrane. And the second one, which is main reason, is variability in the four resistors. While the resistors are processed at the same time, there are some variations. The offset voltage can be compensated by connecting external resistors. It can be compensated using compensating resistors along with electronics.

(3) Nonlinearity

Referring to the output voltage, V_0, versus applied pressure, P, and the endpoint straight line shown in Fig. 14, the nonlinearity NL_i of a pressure sensor at a specific pressure P_i is defined as follows.

$$NL_i = \frac{V_{0i} - \frac{V_{0m}}{P_m}P_i}{V_{0m}} \times 100\% \tag{18}$$

where V_{0i} and V_{om} are the output voltages respectively at a pressure P_i and the full scale

Figure 11: Longitudinal and transverse stress at the centre of the rectangular diaphragm, as a function of its length for fixed.

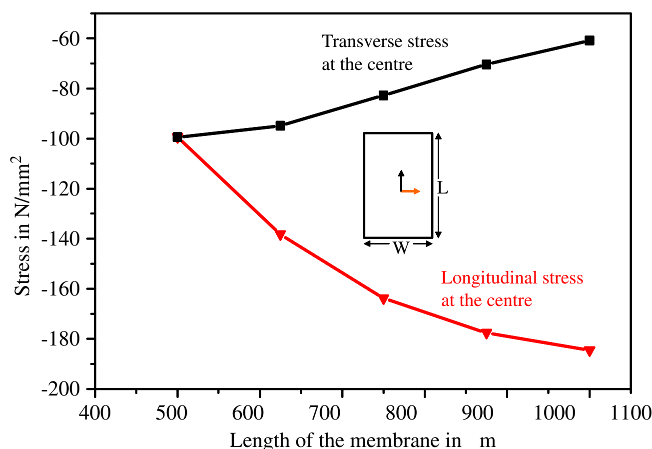

output voltage at the maximum pressure input P_m. Thus, the nonlinearity can be either positive or negative depending upon the calibration point. The nonlinearity of the pressure sensor is the maximum value of NL_i. From Table 4 it can be seen that the nonlinearity is well within 1% in the devices having smaller aspect ratios while the device having aspect ratio 1250/500 shows a nonlinearity of 2.9% and the sensitivity of this device is almost double that of the device with aspect ratio 750/500. These numbers once again illustrate that increasing the $\frac{a}{h}$ ratio enhances the sensitivity and at the same time worsens the linearity considerably.

The nonlinearity in the piezoresitive pressure sensors is caused mainly by two factors, as explained below:

Figure 12: Schematic diagram of the polysilicon piezoresistive pressure sensor.

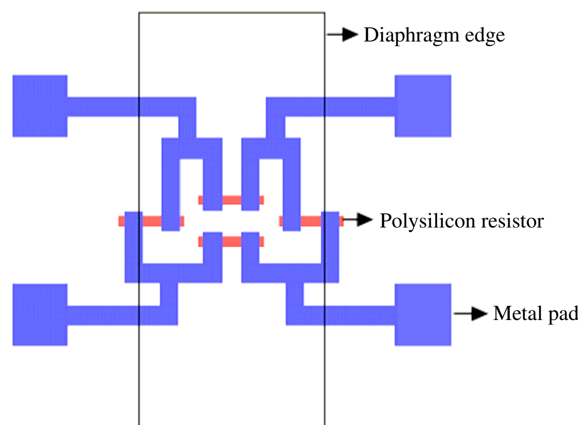

Figure 13: The schematic cross-section of polysilicon piezoresistive pressure sensor.

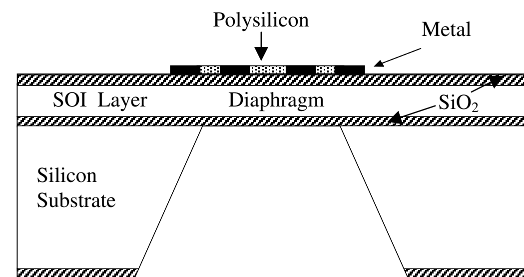

(i) The nonlinear relationship between the stress and the pressure applied. As discussed in section 6.1, if the deflection of the diaphragm is not small compared to its thickness, the central plane of the diaphragm stretches like a balloon. Due to this balloon effect, the diaphragm is subjected to an in-plane stress component, σ_c, in addition to the stress, σ_b caused by the bending of the diaphragm. The stress,σ_b, caused by bending gets reduced in magnitude as the stretch of the diaphragm takes part of the pressure load and this results in the nonlinearity. The nonlinearity caused by the balloon effect (i.e., the stretch) is smaller when the sensor is subjected to pressure from the front side where the resistors are located. This is because σ_c is always positive irrespective of position in the diaphragm and the direction of the applied pressure, whereas the polarity of σ_b can either be positive or negative depending on the position in the diaphragm and the sign of the applied pressure. Thus, both σ_c and σ_b are positive at the diaphragm edge when the pressure is applied from the front side whereas σ_b is negative and σ_c is positive when the pressure is applied from the backside. Hence, when the pressure is applied from the front side the stresses add up and hence the total stress tends to be closer to the linear theory which assumes that the stress distribution is a result of pure bending.

(ii) The piezoresistive coefficient of silicon is generally considered to be independent of the stress. In practice, this is not really true when examined with high accuracy. The nonlinear relationship between the piezoresistive coefficient and the stress is thus another source of nonlinearity in piezoresistive pressure sensors.

(iii) The third cause of the nonlinear output voltage is due to the difference in piezoresistive sensitivity between the resistors of the Wheatstone bridge.

Table 4: Summary of Results on the packaged pressure sensors

Membrane thickness, and aspect ratio	Offset Voltage for 1 Volt input (mV)	Sensitivity (mV/Volt/BAR)	Maximum deviation in the Linearity (%age)
10 μm, 500 μm × 750 μm	8.7	5.81	0.06 up to 3 Bar
10 μm, 500 μm × 1125 μm	8.7	10.3	2.90 up to 3 Bar
15 μm, 500 μm × 875 μm	8.4	1.8	0.36 up to 10 Bar

MOSFET: is the acronym for a semiconductor device Metal Oxide Semiconductor Field Effect Transistor. The gate is the input terminal. Current can flow between the other two terminals called the source and drain when a voltage greater than the threshold voltage is applied to the gate w.r.t. the source.

Threshold Voltage: is the minimum voltage that should be applied to the gate of a MOSFET so that current flows between the other two terminals (source and drain) when a voltage is applied between them.

Differential and common mode, common mode rejection ratio: In the differential mode the same voltage V_G is applied to the two input terminals 1 and 2 as shown in Fig. 16. The voltage gain A_C in this mode should be very low so that the output voltage V_0 is ideally zero when the common voltage appears at the two input terminals In the differential mode the amplifier amplifies the voltage difference between the two input terminals-1 and $2 = .(\Delta V_G + \Delta V_G)$ as shown in Fig. 16 is amplified with a gain A_D. This differential gain should be large so that the voltage difference between the two input terminals gets amplified to result in a larger voltage output V_0 due to the differential input voltage. The common mode rejection ratio is $= A_D/A_C$. This ratio should be very high for a good differential amplifier.

(4) Temperature coefficient of Sensitivity

The output V_0 of a piezoresitive pressure sensor is proportional to the piezoresistive coefficient π of the piezoresistors and in general we can express it in terms of the applied pressure P and supply voltage V_{in} by the equation,

$$V_0 = \frac{\Delta R}{R} V_{in} = cP\frac{a^2}{h^2}\pi V_{in} \tag{19}$$

Here 'c' is a proportionality constant related to the structural design. The piezoresistive coefficient π is a function of temperature and doping concentration and the temperature coefficient of π (TCπ) also is a function of doping. From the relation (19), therefore, the temperature coefficient of sensitivity (TCS) of the pressure sensor is,

$$TCS = TC\pi \tag{20}$$

Generally, $TC\pi$ is found to be negative. Thus, even when the $TC\pi \approx -0.1\%$, sensitivity of the pressure sensor will change by about 5 % when the temperature is raised by 50 °C. Therefore, it is important to compensate the TCS.

One of the simplest ways of compensation is to use a constant current supply I_{in} instead of a constant voltage supply so that the bridge input voltage in the equation (19) is $V_{in} = I_{in}R_B$, and hence the TCS is a function of the temperature coefficient TCR of the bridge resistors and is given by

$$TCS = TC\pi + TCR \tag{21}$$

Here, $TC\pi$ is negative. The TCR depends on the doping concentration and hence it can be adjusted so that TCR is positive values and reduces the TCS. However, with this approach it may be necessary to precisely adjust the doping concentration so that TCR exactly cancels out $TC\pi$. On the other hand, zero TCS can be easily achieved by connecting and adjusting an external resistor R_p (as shown in the Fig. 15) parallel to the sensor bridge circuit provided the TCR of the bridge resistor is higher than the magnitude of $TC\pi$. This method does not require precise adjustment of the doping concentration of the piezoresistors. In practice, the parallel resistor can be replaced by an appropriate electronic circuitry.

Figure 14: Output voltage V_0 versus pressure, P, and the corresponding end-point straight line.

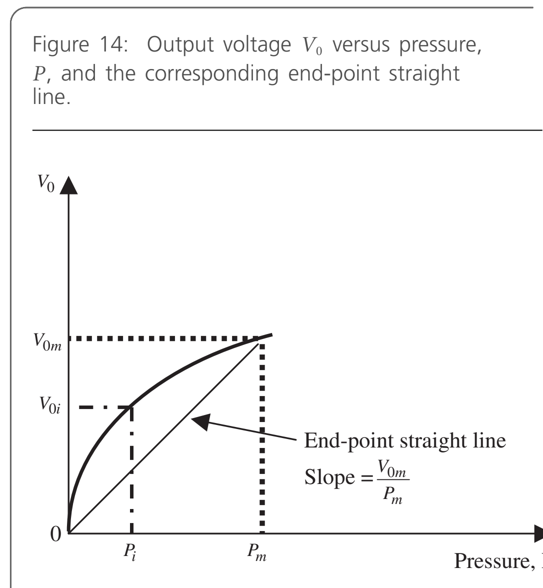

Figure 15: Current source power supply and parallel resistor compensation for TCS

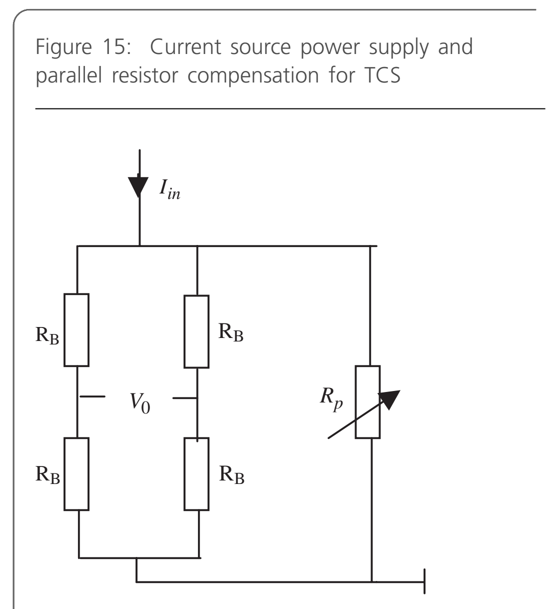

Figure 16: Circuit diagram of the MOSFET source coupled differential amplifier.

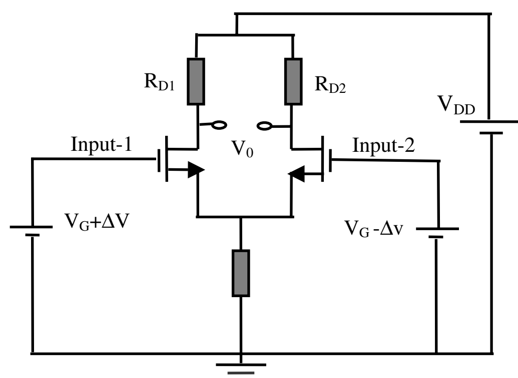

Figure 17: Common mode and differential mode output of the differential amplifier.

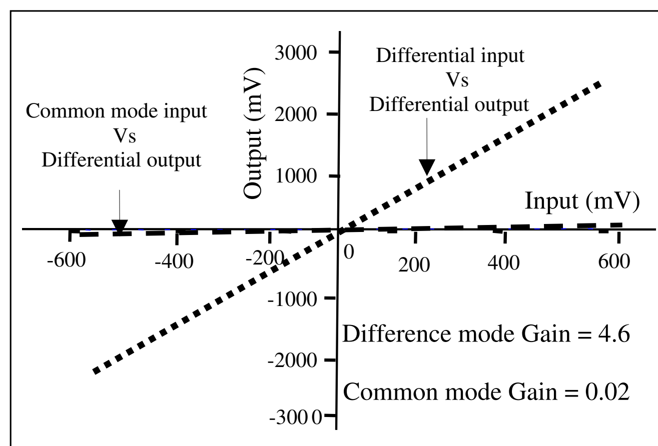

9. MOS integrated piezoresistive pressure sensors[25,26,27]

In this section we demonstrate the benefits of using Silicon On Insulator (SOI) approach for integrating micromachined silicon sensors with electronics. Design and process integration of source-follower amplifier circuit with piezoresistive polysilicon pressure sensor is used for illustrating the merits of the SOI approach. With this approach the SOI layer is used for the diaphragm and its thickness and lateral geometry decides the mechanical properties such as burst pressure and sensitivity. The *doping concentration* controls the electrical characteristics such as the *threshold voltage*, mobility and transconductance of the *MOSFET* in the electronics circuit.

9.1. *Design and fabrication of a Differential Amplifier*

In order to arrive at a process compatible with the process steps of polysilicon piezoresistive pressure sensors described in the previous sections, source coupled differential amplifier configuration shown in Fig. 16 was designed using a circuit simulator for achieving a differential gain of five with supply voltage of 10 V. Based on the simulation results, the resistor values were chosen such that the output varies linearly with the input voltage up to at least 100 mV using MOSFET threshold voltages above 0.5 V. In order to achieve process compatibility with the pressure sensor process, the resistors of the amplifier circuits were designed and process steps were tailored such that they can be fabricated along with the process step of piezoresistors of the sensor. The resistors for the amplifier have been realized using boron-doped polysilicon. The gate electrode for the MOSFET is realized using a heavily phosphorus doped polysilicon. The MOSFETs for the amplifier is fabricated using a 0.6 μm SOI wafer having the film thickness of 0.6 μm. The circuit simulation results have shown that the drain resistor of 10 kΩ, with R_D/R_S equal to 2.5 and threshold voltage of around 500 mV are the desired parameters to obtain a differential voltage gain of 5. The necessary masks to fabricate the differential amplifier are designed using a software called the L-Edit .*The differential mode* and *common mode* characteristics measured on the fabricated differential amplifier are presented in Fig. 17. A *common mode rejection Ratio* of 230 has been achieved with a differential gain of 4.6.

9.2. *Demonstration of MOS Integrated Piezoresistive Pressure Sensor on an SOI Wafer*

The integration of polycrystalline Piezoresistive pressure sensor is demonstrated by the following steps:[27]

(1) After carrying out several process runs, the process suitable for integration of the MOSFET amplifier with the pressure sensor was developed. During this development stage it was also recognized that the integration of electronics with the micromachined sensors is certainly NOT a straightforward task as it is usually believed.

(2) Based on the process that was finally arrived at after several experiments, a set of seven photo masks were designed and fabricated for realizing the pressure sensor integrated monolithically with MOSFET differential circuit shown in Fig. 18. The composite mask layout is shown in Fig. 19.

(3) MOS integrated polycrystalline piezoresistive sensors were next fabricated.

Figure 18: Circuit diagram of MOSFET Integrated pressure sensor.

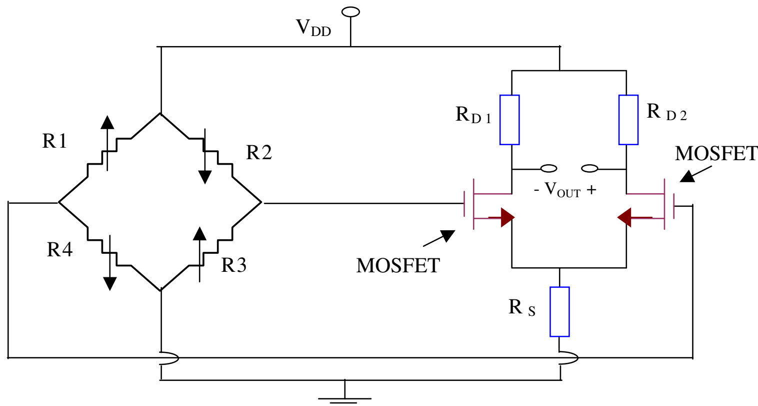

Figure 19: Composite mask layout used to fabricate the integrated pressure sensor

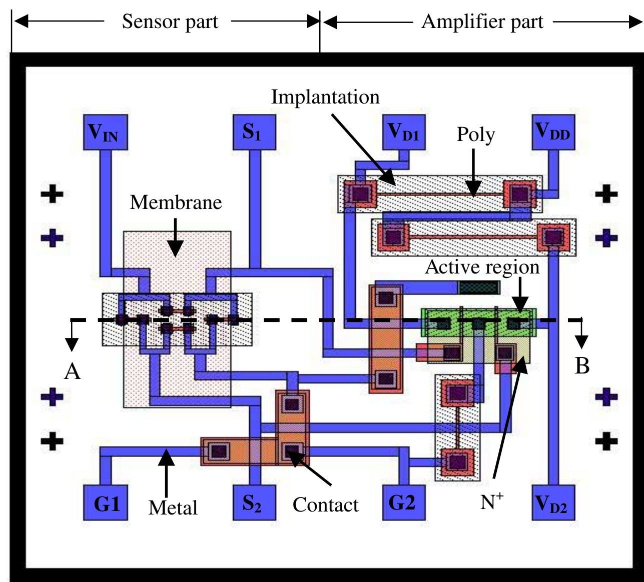

A schematic cross section of the MOSFET integrated Piezoresitive pressure sensor fabricated on SOI wafers with the SOI layer thickness of 11 μm is shown in Fig. 20. The devices were fabricated in the microelectronics laboratory at IIT Madras, Chennai and they were next packaged at BEL, Bangalore and tested at IIT Madras, Chennai. Devices were tested with 10 V supply for the monolithic chip containing the pressure sensor and the amplifier. An output voltage of 0.956 V was obtained with the packaged MOS integrated sensor at 3 bar gauge pressure with 10 V input to the integrated chip. The Integrated sensor showed excellent linearity. For a full scale output of 0.956 V at 3 bar pressure, the maximum nonlinearity of 0.2% has been achieved. Even for a full scale output of 1.59 Volts at 5 bar pressure, the maximum linearity is found to be within 0.3%. The pressure versus output voltage characteristics of the final packaged device are shown in Fig. 21.

10. Closure

(1) The basic concepts and requirements of silicon micromachining have been presented bringing out the importance of silicon as a suitable material for MEMS.

(2) The paper gives a bird's eye view of the different types of pressure sensors and then focuses on the details of the piezoresitive pressure sensors. The concept of piezoresistive coefficient and gauge factor in both single crystal and polycrystalline materials has been addressed in the paper bringing out the difference in the design criteria in single crystal and polycrystalline silicon piezoresistive pressure sensors. The design criteria with flat type and sculptured type diaphragms have been discussed in detail.

(3) A derailed design procedure for piezoresitive pressure sensor has been presented for deciding the thickness, length and width of the diaphragm and the arrangement of both single crystal and polycrystalline silicon resistors on the diaphragm to maximize the sensitivity of the pressure sensor and their relative merits are compared.

(4) The pressure sensors have been fabricated using an SOI wafer approach, with polycrystalline silicon piezoresistive resistors organized in a Wheatstone bridge configuration on the membranes.

(5) The Devices have been packaged using TO39 headers and they have been tested up to a pressure of 10 Bar with nitrogen gas pressure using a specially designed jig. The results have shown excellent linearity in the range of operation proposed to be used. : (a) 0–10 Bar for the devices having membranes of thickness 15 μm and (b) 0–3 Bar for the devices having membranes of thickness 10 μm.

(6) MOSFET Differential Amplifiers have been designed for operation at 10 V power supply and suitable process steps have been evolved to enable integration of these amplifier circuits with the process steps of pressure sensor fabrication.

(7) The feasibility of Integration of polycrystalline silicon pressure sensor with the Source follower MOSFET amplifier has been demonstrated by designing suitable process steps and photo-masks for integrating the sensor and the

Figure 20: Schematic Cross-section at AB of MOSFET Integrated Piezoresistive Pressure Sensor shown in Fig. 19.

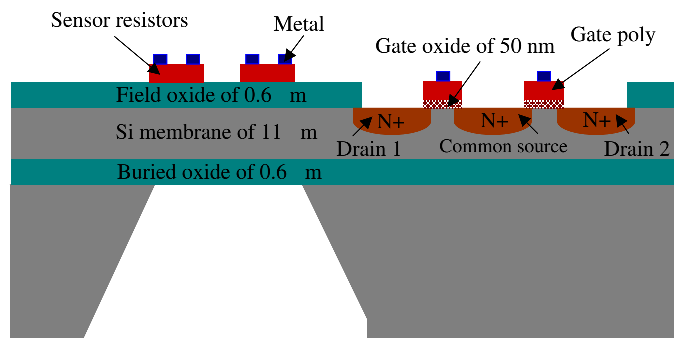

Figure 21: Test results of integrated pressure sensor fabricated on 11 μm SOI wafer.

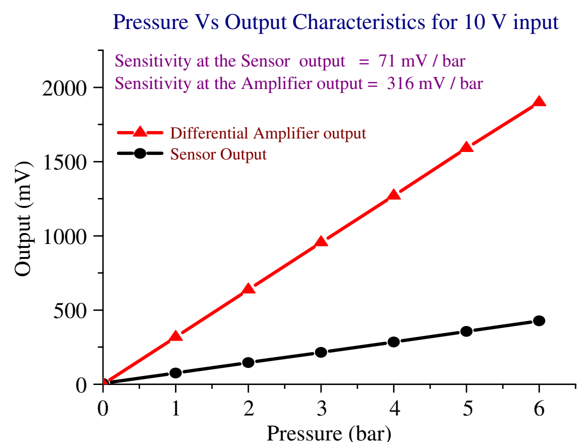

MOSFET amplifier circuit followed by fabrication and testing of the monolithic integrated chip with Silicon On Insulator (SOI) approach. These devices were packaged and tested. An output voltage close to 1.0 V was obtained with the packaged MOS Integrated sensor at three Bar gauge pressure with 10 V input to the integrated chip. The Integrated sensor showed excellent linearity with the maximum nonlinearity of 0.2 percent on a full scale output of 1.0 V at three Bar pressure.

Acknowledgements

The support received from the National Program on Smart Materials (NPSM) and the Project Assessment and Review Committee (PARC)-2 for the continued support, and appreciation by the Chairman and members of the BSMART and PARC-2 is gratefully acknowledged.

Received 30 November 2006; revised 20 January 2007.

References

1. David J. Nagel, ‘MEMS: Micro Technology, Mega Impact’, IEEE Circuits & Devices, Vol. 17, No.2, 14–25, March 2001.
2. C.A. Bang, J.M. Melzak and M. Meherghany, “From microchips to MEMS”, Microlithography world, p.15, spring 1994.
3. B. Sampsell, “The digital micro mirror device and its application to projection displays” The 7th Int Conf. on solid-state sensors and actuators, p.24, Tokohama, Japan, June 1993.
4. Peterson K.E., “Silicon as a mechanical material”. *Proceedings of IEEE*, Vol. **70**, 420–457, 1982,
5. J.P. Sullivan, T.A. Friedmann and K. Hjort, “Diamond and Amorphous Carbon MEMS”, MRS Bulletin, Special Issue on micromechanical Systems: Technology and Application, Vol. 26, No.4, 309-311, April 2001.
6. S.M. Spearing, “Materials issues in Micromechanical Systems (MEMS)”, Acta Matter, Vol. 48, 79–196, 2000.
7. Rob Santilli, ‘Markets for micro engineered products’. *European Semiconductor International*, 19–20, 1995.
8. Gregory T.A. Kovacs, “*Micromachined Transducers sourcebook*”, WCB McGraw-Hill, 1998.
9. Smith C.S., “Piezoresistance Effect in Germanium and Silicon”, *Physical Review*, Vol. 94, 42–49, 1954.
10. P. Kleimaan, B. Semmache, M. Le Berre, and D. Barbier “Stress-dependent hole effective masses and piezoresistive properties of *p*-type monocrystalline and polycrystalline silicon”, *Physical review B*, Vol. 57, No.15, 8966–8971, 1998.
11. M.A. Omar, *Elementary Solid State Physics*, Addison Wesley, 1975.
12. S.M. Sze, Semiconductor sensors, *John Wiley & Sons*, New York, 1994.
13. Nadim Maluf, An introduction to Microelectromechanical systems engineering, Artech house inc., 2000.
14. Yozo Kanda, Piezoresistance effect of silicon, *Sensors and Actuators A*, Vol. 28, 83–91, 1991.
15. V. Mosser, J. Suski, J. Goss and E. Obermeier, Piezoresitive pressure sensors based on Polycrystalline silicon, *Sensors and Actuators*, 28, 113–132, 1991.
16. V.V. Meleshenko, Bending of an elastic rectangular clamped plate: exact versus engineering solutions, J. Elasticity, Vol. 48, 1–50, 1997.
17. J.Y. Pan, P. Lin, F. Maseeh, S.D. Senturia, Verification of FEM analysis of load – deflection methods for measuring mechanical properties of thin films, Proc. Hilton Head workshop, June 4–7, 70–73, 1990.
18. J.R. Mallon, F. Pourahmadi, K. Petersen, Barth T. Vermeulen and Brezek J., Low Pressure Sensors employing bossed diaphragms and precision etch – stopping Sensors and Actuators’ Vol. A21–A23, 89–95, 1990.
19. Min-Hang Bao, Micro Mechanical Transducers: Pressure Sensors, Accelerometers and Gyroscopes. Elsevier, NY, 2000.
20. V. Mosser, J. Suski, J. Goss and E. Obermeier, Piezoresitive pressure sensors based on Polycrystalline silicon, *Sensors and Actuators,* Vol. 28, 113–132 , 1991.
21. Manjula S. Raman, Teweldebhran Kifle, Enakshi Bhattacharya, and K. N. Bhat, Physical Model for the Resistivity and Temperature Coefficient of Resistivity in Heavily Doped Polysilicon. IEEE Transactions on Electron Devices , Vol. 53, No.8 1885–1892, August 2006.
22. Liu Xiaowei, Li Xin, Wang Wei, Wang Xilian, Che Wei, Liu Zhenmao. Computer simulation of polysilicon piezoresistive pressure sensors. IEE conference proceedings, 891–894, 1998.
23. V. Mosser, J. Suski, J. Goss, Piezoresitive Pressure Sensors

based on Polycrystalline Silicon, Sensors and Actuators A, Vol. 28, 113–132, 1991.

24. K.N. Bhat, P.R.S. Rao, E. Bhattachara, A. Dasgupta, N. Dasgupta, V. Vinoth Kumar, K. Sivakumar, S.R. Manjula, S.P. Madhavi, Y. Sushma, R.J. Daniel, Micromachined polysilicon piezoresistive pressure sensor & accelerometer with SOI approach, Electronics Today (India), 65–67, June 2005.
25. K.N. Bhat, V. Vinoth Kumar, K. Sivakumar, S.P. Madhavi, A. DasGupta, P.R.S. Rao, E. Bhattacharya, N. DasGupta, S.R. Manjula, R.J. Daniel and K. Natarajan, Silicon Micromachining for MOS Integrated Piezoresistive pressure Sensors with SOI approach Indo-Japan Joint Seminar on Micro-Nano Manufacturing Science, Tokyo , February 19–26, 2006.
26. V. Vinoth Kumar, MS Thesis entitled Design and Process Optimization for Monolithic Integration of Piezoresistive Pressure Sensor and MOSFET Amplifier with SOI Approach, Electrical Engineering Department, IIT Madras, June 2006.
27. V. Vinoth Kumar, Amitava DasGupta and K.N. Bhat. Process optimization for monolithic integration of piezoresistive pressure sensor and MOSFET amplifier with SOI approach, Journal of Physics, Institute of Physics Publishing, Vol 34, 210–215, 2006

K.N.Bhat received the BE, degree in Electrical Technology from the Indian Institute of Science Bangalore, India, MEng and Ph.D degrees in Electrical Engineering from the Renselaer Polytehnic Institute (RPI) Troy New York and the Indian Institute of Technology Madras. His post doctoral research work at RPI Troy during 1979-1981 involved processing and technology development for polycrystalline thin film GaAs MIS solar cells, and diffused junction GaAs solar cells. He has been actively involved in the teaching and research activities of the Electrical Engineering Department of IIT Madras since 1969 till June 2006. He has taught few courses and taken part in research work in the MEMS area during January 1999 -December 1999, in the EE Department of the University of Washington, Seattle where he was a Visiting Professor on Sabbatical leave from IITM.

His research work at IITM involved modeling and technology of silicon BJTs, MOSFETs , gallium arsenide MESFETs, polycrystalline silicon MOSFETs and grain boundary passivation, nanoscale tunnel oxides on silicon for application in flash memory devices, and MEMS devices such as pressure sensors , accelerometers and silicon micropump . He has been with the ECE Department in the Indian Institute of Science Bangalore since October 2006 as Visiting Professor. He is a Fellow of the Indian National Academy of Engineering.